Available online at www.sciencedirect.com

ScienceDirect

Mendeleev Commun., 2021, **31**, 185–187

Mendeleev Communications

Molecular mechanism of the cesium and rubidium selective binding to the calix[4]arene revealed by Born–Oppenheimer molecular dynamics simulation and electron density analysis

Anna M. Kulakova[a] and Maria G. Khrenova*[a,b]

[a] *Department of Chemistry, M. V. Lomonosov Moscow State University, 119991 Moscow, Russian Federation. E-mail: khrenova.maria@gmail.com*

[b] *A. N. Bach Institute of Biochemistry, Federal Research Centre 'Fundamentals of Biotechnology', Russian Academy of Sciences, 119071 Moscow, Russian Federation*

DOI: 10.1016/j.mencom.2021.03.013

Born–Oppenheimer molecular dynamics simulations with PBE-D3/GTH-DZVP potentials were utilized to explore molecular mechanism of alkali metal cation binding to the calix[4]arene. The calculated standard Gibbs free energy decreased to the higher extent upon binding in case of Cs^+ and Rb^+ compared to Li^+, Na^+ and K^+. The experimentally observed selectivity was attributed to the stronger coordination shells of Cs^+ and Rb^+ in the calixarene-bound state compared with the water-coordinated complexes as revealed by electron density analysis.

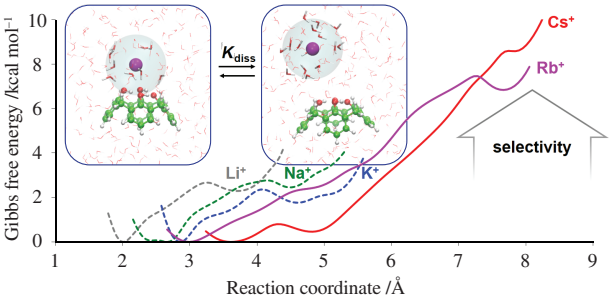

Keywords: calixarene, alkali metal, Born–Oppenheimer molecular dynamics, radiocesium extraction, selectivity.

Environmental contamination by radioactive nuclides is a challenging problem for modern science and technology. Those are accumulated in soils and fluids and selective separation methods should be used to remove radioactive wastes. Among those, a ^{137}Cs isotope is highly presented in soils after nuclear power plant accidents.[1] One of the prospective directions in waste removal is the utilization of macrocyclic compounds that selectively bind a certain type of ions. Processes like solvent extraction and adsorption have been used in large scale applications;[2] for example, caustic-side solvent extraction (CSSX) process is specifically developed to separate cesium from alkaline waste.[3] Calix[4]arenes and their derivatives have broad range of applications including extraction and separation.[4–8] The X-ray data on the structures of metal cation–calixarene complexes in crystals is were reported.[9,10] However, the molecular mechanism of cation binding from the aqueous solution has not been extensively discussed.[11]

In this work, we focus on the molecular mechanism of the selective binding of Rb^+ and Cs^+ cations to calix[4]arene in the presence of other alkali metal cations. Previously, we demonstrated the importance of the *ab initio* potentials in molecular dynamics simulations for proper description of both energetic and entropic contributions of the binding process.[11] Herein, we apply this approach to evaluate binding process for the entire set of the alkali metal cations. We extend our study with the analysis of the electron density in the calix[4]arene-bound state of alkali metal cations and those being surrounded by water molecules to further explore the mechanism of selective binding.

Figure 1 demonstrates a model system composed of a calix[4]-arene molecule and an alkali metal cation surrounded by 291 water molecules forming a rectangular box. We calculated a

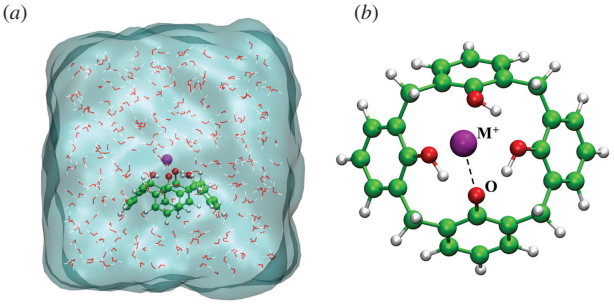

Figure 1 (*a*) The model system of a complex of calix[4]arene with an alkali metal cation solvated in a rectangular water box. (*b*) The reaction coordinate shown by black dashed line. Here and in other figures, carbon, oxygen and hydrogen atoms and an alkali metal cation, M^+, are shown in green, red, white and magenta, respectively.

series of molecular dynamic trajectories with PBE-D3/GTH-DZVP DFT potentials and additional harmonic potentials centered at different values of the reaction coordinate.† We obtained distance distributions between cation and calix[4]arene

† *Computational protocol.* We utilized the model system from ref. 11 and performed simulations with Li^+, K^+ and Rb^+ cations. The model system (Figure 1) for all simulations includes a calix[4]arene with one of the four alcohol groups being deprotonated, an alkali metal cation (Li^+, Na^+, K^+, Cs^+, Rb^+) and 291 water molecules in a rectangular box of ~20 Å size. We used a pre-equilibrated model system from ref. 11. The Born–Oppenheimer molecular dynamics (MD) simulations were performed in the CP2K program package.[14] Model systems were described in the density functional theory approximation with the GGA functional PBE[15] with the empirical dispersion correction D3[16] broader range of applicability, and less empiricism. The main new ingredients are atom-pairwise specific dispersion coefficients and cutoff

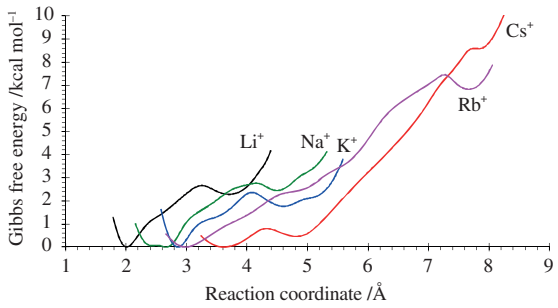

Figure 2 Standard Gibbs energy profiles for alkali metal cations binding to calix[4]arene calculated by umbrella integration method.

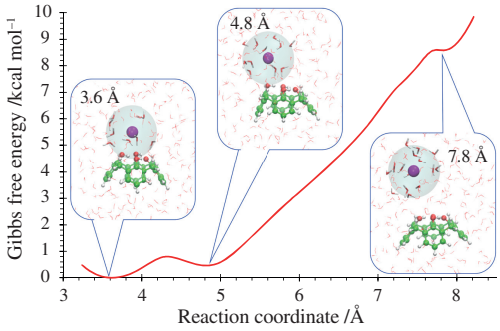

Figure 3 Standard Gibbs free energy profile of cesium cation binding to the calix[4]arene. The insets demonstrate surrounding of the cesium cation at minima.

oxygen atom (reaction coordinate) and used them for the umbrella integration analysis. This allowed us to calculate the standard Gibbs free energy profile of a complex formation from the separate ligand and metal cation species solvated by water molecules. In bound complexes an alkali metal cation (M^+) is located on the top of calix[4]arene cone and forms coordination bonds with the phenyl oxygen atoms of calix[4]arene; the rest of the coordination shell is completed by water molecules. After dissociation, the coordination shell of M^+ is composed of water molecules with the coordination number being different depending on the particular cation.

Figure 2 demonstrates standard Gibbs free energy profiles of M^+ binding to calix[4]arene anion. Profiles for Li^+, Na^+, K^+ and Rb^+ have only two minima corresponding to the bound and unbound states. Values of reaction coordinate corresponding to the bound and dissociated minima increase in the series $Li^+ < Na^+ < K^+ < Rb^+ < Cs^+$ according to the ionic radii (Table 1).

In case of Cs^+ binding, the profile of Gibbs free energy is exceptional in having three minima (Figure 3). The minimum with the smallest reaction coordinate of 3.6 Å corresponds to the bound complex with the coordination shell of Cs^+ being composed of two coordination bonds with the calix[4]arene, and the residual coordination shell is completed with water molecules. The second minimum at 4.8 Å corresponds to the partially bound complex with only one coordination bond between calix[4]arene and Cs^+, while the third minimum at 7.8 Å corresponds to the fully dissociated complex. Upon binding, the coordination shell is saturated sequentially; the coordination bond between the calix[4]arene and Cs^+ is formed first, followed by the formation of second bond further lowering the standard Gibbs free energy of the system.

The standard Gibbs free energies of M^+ binding (Figure 2) are negative for all compounds. System stabilization due to the complex formation increases in the row $K^+ < Na^+ \approx Li^+ << Rb^+ < Cs^+$. The same trend and the similar values of binding free energy ΔG° were observed in experimental studies of cation binding with substituted calixarene in aqueous solution.[12] The Rb^+ and Cs^+ cations bind to calix[4]arene much stronger than Li^+, Na^+ and K^+ cations. The explanation of the selectivity might be the following. For all metal cations, the formation of coordination bond with charged phenolate fragment is more preferable as compared to a neutral H_2O molecule. However, the geometry configuration of the coordination shell is perturbed upon water to calix[4]arene exchange that is more pronounced for smaller cations with smaller coordination numbers.

To further explore the mechanism of selective Cs^+ binding, we performed additional DFT/PBE0/DZP-DKH calculations in molecular clusters composed of alkali metal cation either solvated by 57 water molecules or bound to a calix[4]arene molecule surrounded by 32 water molecules. Figure 4 shows the example of these molecular clusters with the Li^+ cation. The efficiency of binding process is determined by lowering the Gibbs free energy upon formation of the bound state, which is explicitly demonstrated in Figure 2. The Gibbs free energy changes can be divided into entropic and enthalpic contributions. Here, we estimate only the second term that is derived from the changed interactions of a metal cation with its coordination sphere in the bound and unbound states. To quantify these

Table 1 Standard Gibbs free energy of complex formation, ΔG°, dissociation constant, K_{diss}, and structural parameters of calix[4]arene anion complex with alkali metal cations. The selectivity coefficient $K_{M/Cs}$ is calculated as the ratio of $K_{diss}(M^+)$ to $K_{diss}(Cs^+)$.

M^+	ΔG° / kcal mol^{-1}	K_{diss}/ mol dm^{-3}	$K_{M/Cs}$	Reaction coordinate at minima on ΔG° surface /Å	
				Bound complex	Dissociated complex
Li^+	–2.3 ± 0.4	2×10^{-2}	2.5×10^{-5}	2.0	3.7
Na^+	–2.2 ± 0.4	3×10^{-2}	1.7×10^{-5}	2.6	4.8
K^+	–1.0 ± 0.5	2×10^{-1}	2.5×10^{-6}	2.9	4.5
Rb^+	–7.0 ± 0.8	7×10^{-6}	7.1×10^{-2}	3.1	7.5
Cs^+	–8.6 ± 0.6	5×10^{-7}	1	3.6	7.8

radii that were both computed from first principles. The coefficients for new eighth-order dispersion terms were computed using established recursion relations. Combined basis of Gaussian functions and plane waves DZVP with Goedecker–Teter–Hutter pseudopotentials was utilized.[17] All simulations were performed in the NVT ensemble, with the volume preliminary adjusted to the 1 atm pressure at 300 K. The system size is large enough to neglect interactions between the solute molecules in a cell and its periodic copies. These two points allow us to conclude that the energy profile that we obtain is a standard Gibbs energy profile. The binding free energy ΔG° calculated as difference of standard Gibbs free energes between bound and unbound state, can be utilized to evaluate dissociation constants K_{diss} according to the conventional formula $\Delta G^\circ = RT\ln K_{diss}$.

To calculate the Gibbs free energy profile of binding an alkali metal cation to calix[4]arene we used umbrella sampling approach[18] coupled with the umbrella integration method.[19] The reaction coordinate was set as a distance between the alkali metal cation and one of the oxygen atoms of calix[4]arene anion. The biasing harmonic potentials were centered at the certain values of the reaction coordinate. 16 MD simulations with different biasing potentials were performed for the Cs^+ and Rb^+ containing systems and 8 for Li^+, Na^+ and K^+ containing systems. The values of force constants of biasing potentials varied from 2 to 16 kcal mol^{-1} Å^{-2} depending on the curvature of the resulting Gibbs energy profile. Molecular dynamics simulations were performed with a 0.5 fs integration time step with the total length of 10 ps of each MD trajectory. The minima on potential energy surface of the metal cation in calix[4]arene-bound state and coordinated by water molecules were calculated at the DFT/PBE0/DZP-DKH[20,21] level of theory using Firefly QC[22] package partially based on the GAMESS US code.[23]

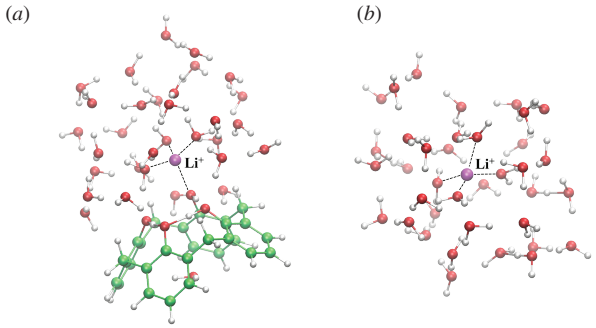

Figure 4 Molecular clusters with Li^+ corresponding to the calix[4]arene (*a*) bound state and (*b*) fully solvated by water molecules. Black dashed lines depict coordination bonds between the alkali metal cation and oxygen atoms of calix[4]arene and water molecules.

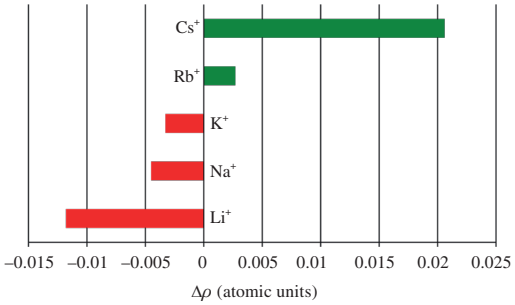

Figure 5 Electron density differences $\Delta\rho$ calculated at BCPs in bound and unbound states. Positive values correspond to the systems with stronger coordination bonds between an alkali metal cation in the complex with a calix[4]arene molecule than in the system with all coordination bonds formed by water molecules.

interactions, we utilized the values of the electron density at the bond critical points (BCPs) obtained within the QTAIM theory.[13] The higher values of the energy density correspond to the stronger interactions. Thus, the stabilization of the bound state should be due to the formation of stronger coordination bonds in the bound state compared with the unbound one. We calculate the sum of electron densities at the BCPs corresponding to the coordination bonds with metal cation in the bound and unbound states. The difference between these two values calculated for the same cation is a quantity that evaluates preferable coordination shell. If it is positive, the bound state is characterized by stronger coordination bonds, thus being more favorable. On the contrary, if this value is negative the unbound state is more preferable (Figure 5). In systems with the Rb^+ and Cs^+ cations the sets of coordination bonds are stronger in the bound state. In case of Li^+, Na^+ and K^+ the coordination shell formed by only water molecules is more preferable.

To conclude, we have calculated Gibbs free energy profiles of alkali metal cation binding to calix[4]arene using Born–Oppenheimer molecular dynamics simulations with DFT PBE-D3/GTH-DZVP potentials. The dissociation constants for Rb^+ and Cs^+ complexes with calix[4]arene are ~10^5 times smaller than those for smaller Li^+, Na^+ and K^+ cations. Electron density analysis of the metal cations complexes with calix[4]arene and in the water-coordinated state has demonstrated that the selective binding of heavy cations is due to the formation of the stronger coordination bonds in the bound states, whereas in case of lighter cations the coordination shell is more stable if formed by water molecules only.

MGK thanks Russian Foundation for Basic Research (project no. 18-03-00605) for the partial support. The study was carried out using the equipment of the shared research facilities of HPC computing resources at M. V. Lomonosov Moscow State University.[24]

Online Supplementary Materials

Supplementary data associated with this article can be found in the online version at doi: 10.1016/j.mencom.2021.03.013.

References

1 G. Steinhauser, A. Brandl and T. E. Johnson, *Sci. Total Environ.*, 2014, **470–471**, 800.
2 J. Wang and S. Zhuang, *Nucl. Eng. Technol.*, 2020, **52**, 328.
3 P. V. Bonnesen, L. H. Delmau, B. A. Moyer and G. J. Lumetta, *Solvent Extr. Ion Exch.*, 2003, **21**, 141.
4 B. S. Creaven, D. F. Donlon and J. McGinley, *Coord. Chem. Rev.*, 2009, **253**, 893.
5 B. Mokhtari, K. Pourabdollah and N. Dalali, *J. Incl. Phenom. Macrocycl. Chem.*, 2011, **69**, 1.
6 *Calixarenes and Beyond*, eds. P. Neri, J. L. Sessler and M.-X. Wang, Springer, Cham, 2016.
7 I. R. Knyazeva, V. V. Syakaev, O. A. Lodochnikova and A. R. Burilov, *Mendeleev Commun.*, 2019, **29**, 700.
8 I. R. Knyazeva, T. P. Gerasimova, I. E. Kolesnikov, V. V. Syakaev, S. A. Katsyuba and A. R. Burilov, *Mendeleev Commun.*, 2020, **30**, 650.
9 F. Pichierri, *J. Radioanal. Nucl. Chem.*, 2017, **311**, 1251.
10 J. M. Harrowfield, M. I. Ogden, W. R. Richmond and A. H. White, *J. Chem. Soc., Chem. Commun.*, 1991, 1159.
11 D. P. Kapusta, Y. I. Meteleshko, I. V. Babchuk and M. G. Khrenova, *Supercomput. Front. Innov.*, 2018, **5**, 70.
12 J.-P. Morel and N. Morel-Desrosiers, *Org. Biomol. Chem.*, 2006, **4**, 462.
13 R. F. W. Bader, *Atoms in Molecules – A Quantum Theory*, Clarendon Press, Oxford, 1990.
14 T. D. Kühne, M. Iannuzzi, M. Del Ben, V. V. Rybkin, P. Seewald, F. Stein, T. Laino, R. Z. Khaliullin, O. Schütt, F. Schiffmann, D. Golze, J. Wilhelm, S. Chulkov, M. H. Bani-Hashemian, V. Weber, U. Borštnik, M. Taillefumier, A. S. Jakobovits, A. Lazzaro, H. Pabst, T. Müller, R. Schade, M. Guidon, S. Andermatt, N. Holmberg, G. K. Schenter, A. Hehn, A. Bussy, F. Belleflamme, G. Tabacchi, A. Glöß, M. Lass, I. Bethune, C. J. Mundy, C. Plessl, M. Watkins, J. VandeVondele, M. Krack and J. Hutter, *J. Chem. Phys.*, 2020, **152**, 194103.
15 J. P. Perdew, K. Burke and M. Ernzerhof, *Phys. Rev. Lett.*, 1996, **77**, 3865.
16 S. Grimme, J. Antony, S. Ehrlich and H. Krieg, *J. Chem. Phys.*, 2010, **132**, 154104.
17 S. Goedecker, M. Teter and J. Hutter, *Phys. Rev. B*, 1996, **54**, 1703.
18 G. M. Torrie and J. P. Valleau, *J. Comput. Phys.*, 1977, **23**, 187.
19 J. Kästner and W. Thiel, *J. Chem. Phys.*, 2005, **123**, 144104.
20 B. P. Pritchard, D. Altarawy, B. Didier, T. D. Gibson and T. L. Windus, *J. Chem. Inf. Model.*, 2019, **59**, 4814.
21 C. Adamo and V. Barone, *J. Chem. Phys.*, 1999, **110**, 6158.
22 A. A. Granovsky, *Firefly version. 7.1.G*, www http://classic.chem.msu.su/gran/firefly/index.html.
23 M. W. Schmidt, K. K. Baldridge, J. A. Boatz, S. T. Elbert, M. S. Gordon, J. H. Jensen, S. Koseki, N. Matsunaga, K. A. Nguyen, S. Su, T. L. Windus, M. Dupuis and J. A. Montgomery, *J. Comput. Chem.*, 1993, **14**, 1347.
24 V. V. Voevodin, A. S. Antonov, D. A. Nikitenko, P. A. Shvets, S. I. Sobolev, I. Y. Sidorov, K. S. Stefanov, V. V. Voevodin and S. A. Zhumatiy, *Supercomput. Front. Innov.*, 2019, **6**, 4.

Received: 8th October 2020; Com. 20/6336